Article

Key Role of Deep Orbitals in the d$_{x^2-y^2}$–d$_{3z^2-r^2}$ Gap in Tetragonal Complexes and 10*Dq*

J. A. Aramburu* and M. Moreno

Cite This: *J. Phys. Chem. A* 2021, 125, 2284−2293

Read Online

ACCESS | Metrics & More | Article Recommendations

ABSTRACT: Using first-principles calculations, we show that the origin of the intrinsic a$_{1g}$($\sim 3z^2 - r^2$)−b$_{1g}$($\sim x^2 - y^2$) splitting, Δ_{int}, in tetragonal transition-metal complexes and the variations of the cubic field splitting, 10*Dq*, with the metal−ligand distance, *R*, are much more subtle than commonly thought. As a main novelty, the key role played by covalent bonding with deep valence ligand levels and thus the inadequacy of too simple models often used for the present goal is stressed. Taking as a guide the isolated D_{4h} CuF$_6^{4-}$ complex, it is proved that Δ_{int} essentially arises from bonding with deep 2s(F) orbitals despite them lying ~ 23 eV below 2p(F) orbitals. This conclusion, although surprising, is also supported by results on octahedral fluoride complexes where the contribution to 10*Dq* splitting from bonding with 2s(F) orbitals is behind its strong *R* dependence, stressing that explanations based on the crystal-field approach are simply meaningless.
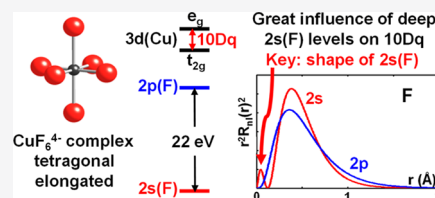
1. INTRODUCTION

A great deal of research is currently focused on transition metal (TM) compounds due to their potential technological interest, witnessed in lasers[1] based on Al$_2$O$_3$:Ti^{3+} or BeAl$_2$O$_4$:Cr^{3+} or devices using manganites.[2] Among insulating TM materials, particular attention is paid to those containing Cu^{2+} ions. Aside from the interest on La$_2$CuO$_4$, the parent compound of high-T_c superconducting cuprates,[3,4] much work is done on Cu^{2+} hybrid perovskites[5−9] currently employed in several devices and on Tutton salts[10−13] containing Cu^{2+} due to their potential application in the study of enzymes. In addition, some Cu^{2+} compounds are responsible for the color of historical pigments[14] or the stained glasses of medieval gothic architecture.[15]

In insulating TM compounds, active electrons are essentially confined in the MX$_N$ complex formed by the TM cation, M, and the N ligands. For this reason, a deep insight into the covalent bonding inside the MX$_N$ unit is crucial for understanding the actual origin of optical and magnetic properties of such compounds following the way started by the pioneering work by Sugano and Shulman.[16,17] The present work is just addressed to prove that subtleties in chemical bonding can play a crucial role for reaching such a goal. Efforts are particularly focused to explain the origin of the dependence on the metal−ligand distances of two relevant splittings of the antibonding orbitals with a mainly d character in MX$_6$ complexes: (1) the splitting 10*Dq* between e$_g$($\sim 3z^2 - r^2$, $x^2 - y^2$) and t$_{2g}$($\sim xy$, xz, yz) levels in octahedral O_h complexes and (2) the splitting Δ between a$_{1g}$($\sim 3z^2 - r^2$) and b$_{1g}$($\sim x^2 - y^2$) levels in tetragonal D_{4h} MX$_6$ units.

For reaching these objectives, the analysis of first-principles calculations and available experimental data is crucial. Indeed, models that use fitting parameters hardly allow one to know the actual microscopic origin of phenomena.[18−20] For this reason, rough approximations such as the superposition[21] or the angular overlap[22] models together with those based on the crystal field (CF) approach are meaningless for the present goal.

In a first step, the present work explores the influence of covalent bonding upon the splitting Δ in tetragonal MX$_6$ units. Positive Δ values mean in this work that a$_{1g}$($\sim 3z^2 - r^2$) has a higher energy than b$_{1g}$($\sim x^2 - y^2$). For clarifying the main ideas, the tetragonal CuF$_6^{4-}$ complex is taken as a guide throughout the present work as Δ has been determined for several compounds containing such a complex. It should be noted here that optical excitations do also depend on the internal electric field induced by the rest of the lattice ions upon the electrons confined in the complex[23−26] and thus there is a contribution to Δ not related to the chemical bonding in the complex.

It is worth noting now that the gap between 2p(F) and 2s(F) valence orbitals of free F atom[27−29] is about 23 eV. Accordingly, it could be expected that Δ is much more influenced by the covalent bonding with shallow 2p(F) than with deep 2s(F) orbitals. We prove in this work that such a guess is not correct as the reality is certainly more subtle.

Table 1. Calculated Intrinsic, Δ_{int}, and Extrinsic, Δ_{ext}, Contributions to the $a_{1g}(\sim 3z^2 - r^2) - b_{1g}(\sim x^2 - y^2)$ Gap, Δ, for Systems Displaying Tetragonal CuF_6^{4-} Units, with $Cu^{2+} - F^-$ Distances R_{eq} and R_{ax} (in Å Units)[a]

system	R_{ax}	R_{eq}	Δ_{int}	Δ_{ext}	$\Delta = \Delta_{int} + \Delta_{ext}$	$|\Delta(exp)|$	refs
$KAlCuF_6$	1.88	2.12	0.68	0.23	0.91	0.83	42,44,45
$CuFAsF_6$	1.84	2.17	0.83	0.36	1.19		44,45
$K_2ZnF_4{:}Cu^{2+}$	1.93	2.04	0.33	0.28	0.61	$\sim$0.70	24,46,52
$Ba_2ZnF_4{:}Cu^{2+}$	1.89	2.07	0.53	0.40	0.93	0.80	24,47
$KZnF_3{:}Cu^{2+}$	2.10	1.97	$-$0.36	$\sim$0	$-$0.36	<0.5	24,31,52

[a]All energies are given in eV units. When $R_{ax} < R_{eq}$, the ground state has a hole in $a_{1g}(\sim 3z^2 - r^2)$ and the extrinsic contribution tends to enhance the value of the intrinsic one. By contrast, for Cu^{2+} doped into the cubic perovskite $KZnF_3$, displaying an elongated equilibrium geometry, the hole in the ground state lies in $b_{1g}(\sim x^2 - y^2)$ and thus the sign of Δ_{int} is negative. The total calculated gap, $\Delta = \Delta_{int} + \Delta_{ext}$, is compared to available experimental data. The values of R_{ax} and R_{eq} metal–ligand distances are taken from experimental data for pure compounds and from calculations for systems where Cu^{2+} enters as an impurity.

Tetragonal complexes are observed for Cu^{2+}-doped cubic lattices[30−33] as a result of the so-called static Jahn−Teller effect,[34−36] a phenomenon ultimately due to the unavoidable presence of random strains in any real crystal.[34] Tetragonal CuF_6^{4-} units are also formed in Cu^{2+}-doped K_2ZnF_4 or Ba_2ZnF_6-layered perovskites though there is no Jahn−Teller effect as the $a_{1g}(\sim 3z^2 - r^2)$ and $b_{1g}(\sim x^2 - y^2)$ levels are not degenerate following the *tetragonal* symmetry of the host lattice.[24] Accordingly, the theory describing the Jahn−Teller effect[34,35] cannot, in general, be transferred[4,9,24] to understand pure layered compounds such as the orthorhombic K_2CuF_4 or Cs_2AgF_4.[37,38] Nevertheless, the Jahn−Teller framework is still surprisingly applied[39−41] to d^9 ions under tetragonal or lower symmetries.

Compressed tetragonal CuF_6^{4-} units are formed in $KAlCuF_6$ or $CuFAsF_6$ pure compounds[42−45] in addition to Cu^{2+}-doped crystals.[24,46−48] By contrast, in CuF_2 or A_2CuF_4 (A = K, Na), the tetragonally compressed CuF_6^{4-} units undergo an *additional* orthorhombic distortion, favored by the existence of adjacent complexes which share F^- ligands.[9,48,49] An orthorhombic instability also takes place in copper Tutton salts[12] and in $NH_4Cl{:}CuCl_4(H_2O)_2^{2-}$.[50,51]

The interest in the Δ gap relies on the fact that it is often the lowest optical excitation of compounds[52] with tetragonal MX_6 units (M = Cu, Ag). Also, in superconductor oxocuprates, the transition temperature, T_c, has been related to the magnitude of the Δ splitting.[53]

In a second step, the present work is devoted to clarify quantitatively the origin of the sensitivity of $10Dq$ to variations of the metal−ligand distance, R, in octahedral complexes. Experimentally, it has been found that $10Dq$ depends on R^{-t}, where the exponent t is often found to be close to 5.[54] By this reason, it is still claimed that the exponent t mainly comes from the CF contribution[40,55] despite this approach leading to $10Dq$ values much smaller than experimental ones.[54]

Seeking to shed light on these issues, in addition to investigating the relation between covalent bonding and the splitting Δ, we have carried out first-principles calculations on tetragonal CuF_6^{4-} units at different values of axial (R_{ax}) and equatorial (R_{eq}) metal−ligand distances. In this analysis, particular attention is paid to explore how the charge on ligands is modified by varying the R_{ax} and R_{eq} distances. In a further step, we analyze in octahedral complexes how the variations of chemical bonding with the metal−ligand distance, R, are quantitatively related to the exponent t.

This work is organized as follows. A brief account of computational tools is given in Section 2 while Section 3 first deals with the two contributions to optical transitions for a TM

complex in an insulating compound: the intrinsic one associated with the isolated complex and the extrinsic one due to the internal electric field created by the rest of the lattice ions.[23,24] That section also deals with the relation between the splitting, Δ, and the variation of charge on ligands. The main results of this work are discussed in Section 4. Special attention is paid in that section to clarify the different influences of bonding with $2p(F)$ and $2s(F)$ orbitals upon the splitting Δ (Section 4.1) of isolated CuF_6^{4-} units and also the origin of the dependence of $10Dq$ on the metal−ligand distance for octahedral complexes (Section 4.2). For the sake of completeness, the reasons behind the similarities and differences between $2p(F)$ and $2s(F)$ orbitals are discussed in Section 4.3. Finally, the applicability of the present ideas to complexes involving Cl^-, Br^-, or O^{2-} as ligands is briefly dealt with in the last section.

2. COMPUTATIONAL METHODS

Ab initio density functional theory (DFT) calculations on *isolated* CuF_6^{4-} complexes have been performed at fixed metal−ligand distances by means of the 2017.03 version of the Amsterdam density functional code.[69] By means of this kind of calculations, we can already explore the dependence of the intrinsic contribution Δ_{int} to the Δ gap upon metal−ligand distances. In these DFT calculations, we have used the popular B3LYP hybrid functional (including 25% of Hartree−Fock exchange[70]) in the spin-restricted and spin-unrestricted Kohn−Sham formalism of the DFT and high-quality all-electron basis sets of triple-ζ plus polarization type. We have verified that similar results are obtained using other hybrid functionals such as the nonempirical PBE0 one.[71]

3. INFLUENCE OF COVALENT BONDING UPON THE Δ SPLITTING IN TETRAGONAL COMPLEXES: A GENERAL VIEW

Although in insulating compounds containing TM cations, active electrons are localized in the MX_N complex, the optical properties cannot, in general, be explained considering only that isolated unit. Indeed, the localized electrons lying in the MX_N complex are *also* subject to the electric field, $\mathcal{E}_R(r)$, created by the rest of the lattice ions, which usually has a perturbative character.[23] By this reason, the energy, E, of an electronic transition can be divided in two contributions[24]

$$E = E_{int} + E_{ext} \tag{1}$$

where E_{int} is the intrinsic contribution to the *isolated* MX_N complex at equilibrium geometry while the extrinsic one, E_{ext}, accounts for the effects of the internal electric field, $\mathcal{E}_R(r)$,

upon the confined electrons. As an example, the intrinsic contribution for $10Dq$ in ruby and emerald[23,56] is the same ($10Dq_{int} = 2$ eV), reflecting the identical $Cr^{3+}-O^{2-}$ distance (1.97 Å) in both gemstones.[23,57,58] Thus, the difference between the red ruby and the green emerald simply arises from the distinct shape of the extrinsic $\mathcal{E}_R(\mathbf{r})$ field in the two gemstones, leading to the small corrections $10Dq_{ext} = 0.24$ eV for ruby and $10Dq_{ext} = -0.05$ eV for emerald.[23,56] In the same vein, the color of the Egyptian blue pigment[14] is just the result of a 0.90 eV shift induced by $\mathcal{E}_R(\mathbf{r})$ on the highest d–d transition of the square-planar CuO_4^{6-} chromophore in $CaCuSi_4O_{10}$.

An insight into the Δ gap between $a_{1g}(\sim 3z^2 - r^2)$ and $b_{1g}(\sim x^2 - y^2)$ levels of tetragonal complexes thus requires taking into account both the intrinsic, Δ_{int}, and extrinsic, Δ_{ext}, contributions. For the sake of clarity, the values of both contributions derived for systems with tetragonal CuF_6^{4-} units are displayed in Table 1. It is worth noting that the existence of an internal electric field allows one to understand why the hole in $KAlCuF_6$[45] and $K_2ZnF_4:Cu^{2+}$[52] is in the $a_{1g}(\sim 3z^2 - r^2)$ orbital in contrast to Cu^{2+} doped into the cubic perovskites $KZnF_3$ or $CsCdF_3$ where it resides in $b_{1g}(\sim x^2 - y^2)$ due to a static Jahn–Teller effect.[30,32] Indeed, for d^9 ions under an initial octahedral symmetry, the existence of a static Jahn–Teller effect usually leads to elongated complexes[34,35] with the exception of $CaO:Ni^+$, a matter dealt with in refs 59 and 60. The extrinsic contribution arising from a tetragonal internal field in $K_2ZnF_4:Cu^{2+}$ and $Ba_2ZnF_4:Cu^{2+}$ also explains why $|\Delta|$ has been detected[46,52] in the 0.6–1 eV region, whereas for $KZnF_3:Cu^{2+}$ it should be below 0.5 eV,[31,52] a fact that concurs with the cubic symmetry of the host lattice. Bearing these facts in mind, the chemical bonding inside the complex essentially influences the intrinsic component, Δ_{int}, of the total gap.

Let us consider an isolated MX_6 unit with a small tetragonal distortion depicted in Figure 1. This condition just implies
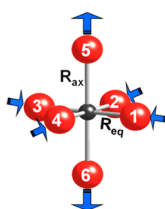

Figure 1. Description of a tetragonally elongated CuF_6^{4-} complex.

that, if R_{ax} and R_{eq} are the two metal–ligand distances, with a mean value $R_m = (R_{ax} + 2R_{eq})/3$, it must be verified that

$$\eta \equiv |(R_{ax} - R_{eq})/R_m| \ll 1 \qquad (2)$$

where η reflects the tetragonal distortion from an octahedral MX_6 complex with a metal–ligand distance equal to the mean value R_m.

The condition given by eq 1 is well followed by all systems of Table 1 involving CuF_6^{4-} units, where $\eta < 0.16$. As Δ_{int} should always be zero when $R_{ax} = R_{eq}$; then it is function of $R_{ax} - R_{eq}$ and can be written in a good first approximation as[45,49,52]

$$\Delta_{int} = \beta(R_m)(R_{eq} - R_{ax}) \qquad (3)$$

where the $\beta(R_m)$ quantity only depends on the R_m value. Previous studies on systems[45,49,52] with tetragonal CuF_6^{4-} units lead to a value $\beta \cong 2.7$ eV/Å when $R_m \cong 2.05$ Å. It should be remarked that eq 3 is valid for systems displaying a static Jahn–Teller effect (like $KZnF_3:Cu^{2+}$) as well as for those whose ground state is determined by the internal electric field,[45] such as it happens for $CuFAsF_6$ or $K_2ZnF_4:Cu^{2+}$. Therefore, the β quantity is *common* to all systems with tetragonal CuF_6^{4-} units provided $R_m \cong 2.05$ Å.

In the rough CF approach, where ligands are treated as point charges, the electrostatic potential due to ligands, V_M, *around* the central cation (placed at $\mathbf{r} = 0$) involves two contributions[61]

$$V_M(\mathbf{r}) = V_M^0 + V_M^{NC}(\mathbf{r}) \qquad (4)$$

Here, V_M^0 is independent of the electronic coordinate, $\mathbf{r}$, but plays a key role for placing the energy of 3d levels of Cu^{2+} above that of 2p(F) ligand levels.[61] Thus, within the CF framework, the non-constant contribution $V_M^{NC}(\mathbf{r})$ is the only one responsible for the splitting Δ_{int} when $R_{eq} \neq R_{ax}$. Accordingly, the gap, $\Delta_{int}(CF)$, for an isolated CuF_6^{4-} unit, derived from the simple CF approach, is given by[17]

$$\Delta_{int}(CF) = |Z_L|e^2[-(8/7)\langle r_d^2\rangle(R_{eq}^{-3} - R_{ax}^{-3})$$
$$- (10/21)\langle r_d^4\rangle(R_{eq}^{-5} - R_{ax}^{-5})] \qquad (5)$$

where $\langle r_d^2\rangle = 1.044$ a.u. and $\langle r_d^4\rangle = 2.674$ a.u. correspond to *free* Cu^{2+} ions[62] and Z_L is the ligand charge. Using these values, $R_m = 2.05$ Å, and even fully neglecting covalency, assuming $Z_L = -1$, we obtain from eqs 3 and 5 that $\beta(CF) = 0.90$ eV/Å, which is three times smaller than the value $\beta \cong 2.7$ eV/Å corresponding to CuF_6^{4-} at $R_m = 2.05$ Å. This comparison strongly suggests that the intrinsic contribution, Δ_{int}, is greatly due to the covalent bonding inside the CuF_6^{4-} unit. In the same way, the experimental $10Dq$ value of octahedral TM complexes is much higher than that calculated under the CF approach provided the right $\langle r_d^4\rangle$ quantity is employed.[54,61]

For understanding the role played by chemical bonding upon Δ_{int}, it is useful to explore how the energy levels are modified as far as we increase the size of the basis set, following an approach first proposed by Löwdin.[63,64] In the present case, let us start with a basis set which includes only the two purely d-wavefunctions of the central cation that are degenerate under an octahedral symmetry $|d_a\rangle = |3z^2 - r^2\rangle$ and $|d_b\rangle = |x^2 - y^2\rangle$. Although in this first step there is no chemical bonding in the two $a_{1g}(\sim 3z^2 - r^2)$ and $b_{1g}(\sim x^2 - y^2)$ levels, their energy is

Table 2. Description of Antibonding Molecular Orbitals for Isolated Tetragonal CuF_6^{4-} Units[a]

Cu^{2+}	F ligands	χ_p	χ_s
$3z^2 - r^2$	equatorial	$-1/2\{p_\sigma(1) + p_\sigma(2) + p_\sigma(3) + p_\sigma(4)\}$	$-1/2\{s(1) + s(2) + s(3) + s(4)\}$
	axial	$(1/\sqrt{2})\{p_\sigma(5) + p_\sigma(6)\}$	$(1/\sqrt{2})\{s(5) + s(6)\}$
$x^2 - y^2$	equatorial	$1/2\{p_\sigma(1) - p_\sigma(2) + p_\sigma(3) - p_\sigma(4)\}$	$1/2\{s(1) - s(2) + s(3) - s(4)\}$

[a]χ_p and χ_s mean ligand wavefunctions hybridized with $3z^2 - r^2$ and $x^2 - y^2$ orbitals of the central cation involving linear combinations of 2p(F) and 2s(F) orbitals, respectively. The positions of six ligand ions are shown in Figure 1.

significantly raised by the repulsive interaction of electrons with the negatively charged ligands involved in the V_M^0 term of eq 4. Also, in this step, the associated energies, E_a and E_b, of $a_{1g}(\sim 3z^2 - r^2)$ and $b_{1g}(\sim x^2 - y^2)$ levels can be written as

$$E_a = E_d + \varepsilon_a^1; \qquad E_b = E_d + \varepsilon_b^1 \qquad (6)$$

where E_d corresponds to the octahedral situation ($R_{ax} = R_{eq}$), while the corrections ε_a^1 and ε_b^1 are not strictly equal due to small CF effects under tetragonal symmetry. Indeed, in this first step $\Delta_{int} \cong \varepsilon_b^1 - \varepsilon_a^1$ whose expression is just given by eq 5.

In a second step, the ligand 2p and 2s wavefunctions are introduced in the basis set and then there is a change of both energy and shape of wavefunctions following the allowed 3d(TM)−2p(F) and 3d(TM)−2s(F) admixtures and the formation of antibonding orbitals. The linear combinations of $2p_\sigma$ and 2s wavefunctions involving axial and equatorial ligands and transforming like a_{1g} and b_{1g} are shown on Table 2. In the case of the a_{1g} irreducible representation, there are two contributions termed as $\chi_j^{eq}(a)$ and $\chi_j^{ax}(a)$ (j = pσ, s), which can be mixed with $d_a = 3z^2 - r^2$, while $d_b = x^2 - y^2$ can only be hybridized with the linear combinations $\chi_j^{eq}(b)$ (j = pσ, s) of equatorial ligands.

Accordingly, in this second step, the normalized $|a_{1g}(\sim 3z^2 - r^2)\rangle$ and $|b_{1g}(\sim x^2 - y^2)\rangle$ wavefunctions have the form

$$|a_{1g}(\sim 3z^2 - r^2)\rangle = N_a|3z^2 - r^2\rangle - \sum_j \lambda_j^{eq}(a)|\chi_j^{eq}(a)\rangle$$
$$- \sum_j \lambda_j^{ax}(a)|\chi_j^{ax}(a)\rangle \qquad j = p\sigma, \ s$$

$$|b_{1g}(\sim x^2 - y^2)\rangle = N_b|x^2 - y^2\rangle - \sum_j \lambda_j^{eq}(b)|\chi_j^{eq}(b)\rangle \qquad (7)$$

Although the $\lambda_j^{eq}(a)$, $\lambda_j^{ax}(a)$, and $\lambda_j^{eq}(b)$ quantities are independent under D_{4h} symmetry ($R_{eq} \neq R_{ax}$), this is no longer true in the octahedral limit as they are related by the conditions

$$\lambda_j^{eq}(b) = \mu_j; \qquad \lambda_j^{ax}(a) = (\sqrt{2}/\sqrt{3})\mu_j;$$
$$\lambda_j^{eq}(a) = (1/\sqrt{3})\mu_j \qquad j = p\sigma, \ s \qquad (8)$$

It is worth noting that although wavefunctions such as $|x^2 - y^2\rangle$ and $|\chi_j^{eq}(b)\rangle$ (j = pσ, s) are not orthogonal, the associated overlap integrals $S_{p\sigma} = \langle x^2 - y^2|\chi_{p\sigma}^{eq}(b)\rangle$ and $S_s = \langle x^2 - y^2|\chi_s^{eq}(b)\rangle$ are both only of the order of 0.1 at equilibrium[65] for MF_6^{4-} complexes (M = Cu, Ni, Co, Fe). For this reason, the total electronic charges $q_{p\sigma}^{eq}(b)$ and $q_s^{eq}(b)$ transferred from the central cation to $2p\sigma$ and 2s orbitals of equatorial ligands in the antibonding $|b_{1g}(\sim x^2 - y^2)\rangle$ orbital are reasonably given by

$$q_{p\sigma}^{eq}(b) = [\lambda_{p\sigma}^{eq}(b)]^2; \qquad q_s^{eq}(b) = [\lambda_s^{eq}(b)]^2 \qquad (9)$$

Similarly, the charges, $q_j^{ax}(a)$ and $q_j^{eq}(a)$ (j = pσ, s) transferred to axial and equatorial ligands in the antibonding $|a_{1g}(\sim 3z^2 - r^2)\rangle$ orbital can be approximated by

$$q_j^{ax}(a) = [\lambda_j^{ax}(a)]^2; \qquad q_j^{eq}(a) = [\lambda_j^{eq}(a)]^2 \qquad (10)$$

In the present step, the values of orbital energies and the 3d−2p and 3d−2s admixtures come from the solution of the secular equation

$$|h_{ik} - ES_{ik}| = 0 \qquad (11)$$

If we now work in second-order perturbations, the energy variations, ε_a^2 and ε_b^2, induced by chemical bonding upon the $|a_{1g}\rangle$ and $|b_{1g}\rangle$ orbitals can be approximated by

$$\varepsilon_a^2 = \frac{\langle d_a|h - E_d|\chi_{p\sigma}^{ax}(a)\rangle^2}{E_d - E_p} + \frac{\langle d_a|h - E_d|\chi_{p\sigma}^{eq}(a)\rangle^2}{E_d - E_p}$$
$$+ \frac{\langle d_a|h - E_d|\chi_s^{ax}(a)\rangle^2}{E_d - E_s} + \frac{\langle d_a|h - E_d|\chi_s^{eq}(a)\rangle^2}{E_d - E_s}$$

$$\varepsilon_b^2 = \frac{\langle d_b|h - E_d|\chi_{p\sigma}^{eq}(b)\rangle^2}{E_d - E_p} + \frac{\langle d_a|h - E_d|\chi_s^{eq}(a)\rangle^2}{E_d - E_s} \qquad (12)$$

Here, $E_d - E_p$ and $E_d - E_s$ stand for the separation between the 3d levels of the central cation and the 2p and 2s levels of ligands in the complex. From the present calculations for CuF_6^{4-} at $R_m = 2.05$ Å, it is found that $E_d - E_p \cong 6$ eV while $E_d - E_s \cong 26$ eV.

Thus, if Δ_{int} is mainly governed by the different chemical bonding in $|a_{1g}\rangle$ and $|b_{1g}\rangle$ orbitals, then

$$\Delta_{int} \cong \varepsilon_a^2 - \varepsilon_b^2 \qquad (13)$$

In the same vein, within the second-order perturbation approach, the covalency parameters $\lambda_j^{eq}(a)$, $\lambda_j^{ax}(a)$, and $\lambda_j^{eq}(b)$ are given by

$$\lambda_{p\sigma}^{ax}(a) = \frac{\langle d_a|h - E_d|\chi_{p\sigma}^{ax}(a)\rangle}{E_d - E_p};$$

$$\lambda_{p\sigma}^{eq}(a) = \frac{\langle d_a|h - E_d|\chi_{p\sigma}^{eq}(a)\rangle}{E_d - E_p};$$

$$\lambda_s^{ax}(a) = \frac{\langle d_a|h - E_d|\chi_s^{ax}(a)\rangle}{E_d - E_s};$$

$$\lambda_s^{eq}(a) = \frac{\langle d_a|h - E_d|\chi_s^{eq}(a)\rangle}{E_d - E_s};$$

$$\lambda_{p\sigma}^{eq}(b) = \frac{\langle d_b|h - E_d|\chi_{p\sigma}^{eq}(b)\rangle}{E_d - E_p};$$

$$\lambda_s^{eq}(b) = \frac{\langle d_b|h - E_d|\chi_s^{eq}(b)\rangle}{E_d - E_s} \qquad (14)$$

Thus, bearing eqs. 1, 7, 8, and 10−12 in mind, Δ_{int} can finally be related to the charges transferred to $2p\sigma$ and 2s ligand orbitals as follows

$$\Delta_{int} \cong \Delta_{int}(p\sigma) + \Delta_{int}(s)$$
$$\Delta_{int}(p\sigma) = (E_d - E_p)[Q_{p\sigma}(a) - Q_{p\sigma}(b)]$$
$$\Delta_{int}(s) = (E_d - E_s)[Q_s(a) - Q_s(b)] \qquad (15)$$

where

$$Q_j(a) = q_j^{ax}(a) + q_j^{eq}(a) \qquad j = p\sigma, \ s$$

$$Q_j(b) = q_j^{eq}(b) \qquad j = p\sigma, \ s \qquad (16)$$

Therefore, according to eq 15, there are two contributions to the gap Δ_{int} reflecting the bonding with $2p\sigma$ and 2s ligand

Table 3. Charges Transferred to Ligands Calculated for an Isolated CuF_6^{4-} Complex at Different Equatorial and Axial Metal–Ligand Distances, R_{eq} and R_{ax}, But *Keeping* the Same Value of the Mean Distance $R_m = (R_{ax} + 2R_{eq})/3 = 2.05$ Å[a]

	$R_{eq} = 2.05$ Å, $R_{ax} = 2.05$ Å	$R_{eq} = 2.00$ Å, $R_{ax} = 2.15$ Å	$R_{eq} = 1.95$ Å, $R_{ax} = 2.25$ Å	$R_{eq} = 2.10$ Å, $R_{ax} = 1.95$ Å
$q_{p\sigma}^{ax}(a)$	0.148	0.148	0.147	0.142
$q_{p\sigma}^{eq}(a)$	0.074	0.068	0.062	0.082
$q_{p\sigma}^{eq}(b)$	0.222	0.225	0.227	0.219
$Q_{p\sigma}(a) - Q_{p\sigma}(b)$	0	−0.009	−0.018	0.005
$\Delta_{int}(p\sigma)$ (eV)	0	−0.06	−0.12	0.03
$q_s^{ax}(a)$	0.023	0.026	0.028	0.025
$q_s^{eq}(a)$	0.010	0.002	0	0.016
$q_s^{eq}(b)$	0.033	0.041	0.051	0.025
$Q_s(a) - Q_s(b)$	0	−0.013	−0.033	0.016
$\Delta_{int}(s)$ (eV)	0	−0.34	−0.86	0.42
Δ_{int} (eV)	0	−0.42	−0.84	0.42

[a]Results are reported for both $a_{1g}(\sim 3z^2 - r^2)$ and $b_{1g}(\sim x^2 - y^2)$ orbitals. The contributions $\Delta_{int}(p\sigma)$ and $\Delta_{int}(s)$ to the energy gap Δ_{int}, derived from the $Q_{p\sigma}(a) - Q_{p\sigma}(b)$ and $Q_s(a) - Q_s(b)$ quantities, are also shown. It can be noted that the value of $\Delta_{int}(p\sigma) + \Delta_{int}(s)$ is close to the gap, Δ_{int}, obtained in a DFT calculation for every value of R_{eq} and R_{ax}.

orbitals. That gap should be zero when the CuF_6^{4-} unit is perfectly octahedral ($R_{eq} = R_{ax}$) and in fact eq 15, in conjunction with eqs 8−10, leads to $\Delta_{int} = 0$ in such a limiting case. Furthermore, eq 15 stresses that the gap, Δ_{int}, is associated with variations of ligand charges on passing from an octahedral situation ($\eta = 0$) to a tetragonal one where $R_{eq} \neq R_{ax}$, a view consistent with the general Hohenberg−Kohn theorem.[66] Indeed, the change of octahedral to tetragonal symmetry implies modifications of the electron−nuclei interactions (the so-called *external potential* in DFT[66]) and necessarily of the associated electronic density. This change in the electronic density is then reflected on variations of ligand charges.

As the present analysis is based on a second-order perturbation approach, its validity requires that in a level like $|b_{1g}(\sim x^2 - y^2)\rangle$ the charges $q_{p\sigma}^{eq}(b)$ and $q_s^{eq}(b)$ transferred to ligands are clearly smaller that the unity. The condition $q_{p\sigma}^{eq}(b) \ll 1$ is better accomplished for fluoride than chloride or bromide complexes due to the higher electronegativity of fluorine (3.9) when compared to that of Cl (3.0) or Br (2.8). By contrast, the condition $q_s^{eq}(b) \ll 1$ is much better fulfilled for all kinds of complexes due to the deep character of 2s(F), 3s(Cl), or 4s(Br) levels of free atoms.[61] For instance, the present calculations for CuF_6^{4-} units, discussed in the next section, give $q_{p\sigma}^{eq}(b) < 0.23$, while a much lower value, $q_s^{eq}(b) < 0.06$, is obtained for the charge transferred to 2s orbitals. This relevant fact also stresses the perturbative character of the 3d−2s admixture.

The present approach focused on the Δ_{int} gap of tetragonal units has also been employed for understanding the intrinsic and dominant contribution to the $10Dq$ value of octahedral complexes and its dependence upon the metal−ligand distance.[67] Interestingly, in the case of octahedral CrX_6^{3-} complexes (X = F, Cl, Br, I), it has been found[67] that the charge transferred to the valence ns level of ligands (n = 2, 3, 4, and 5 for F, Cl, Br, and I, respectively) in the antibonding $e_g(\sigma)$ orbital is always smaller than 0.1.

For the sake of clarity, when $\eta \neq 0$ the Cu-wavefunction of the $|a_{1g}\rangle$ orbital is not a purely $3z^2 - r^2$ orbital as it involves a small admixture (~1%) of 4s(Cu). For elongated complexes, that admixture tends to enhance the electronic density of axial ligands, a matter discussed in ref 68. For obtaining such a 3d(Cu)−4s(Cu) hybridization in the present scheme, it is however necessary to go beyond the second-order approach.

4. RESULTS AND DISCUSSION

4.1. Ligand Charges and Δ Gap for Isolated CuF_6^{4-} Units: Influence of the Tetragonal Distortion. DFT calculations on the isolated CuF_6^{4-} unit have been carried out using the transition state configuration $a_{1g}^{1.5}b_{1g}^{1.5}$, varying the equatorial and axial metal−ligand distances but maintaining the mean distance $R_m = 2.05$ Å. This allows one to calculate the Δ_{int} gap simply by means of the Janak theorem[66] and to determine the charges transferred to 2pσ and 2s ligand orbitals for both a_{1g} and b_{1g} levels. Indeed, the use of the *average* $a_{1g}^{1.5}b_{1g}^{1.5}$ configuration allows one to establish a reasonable link with the analysis carried out in Section 3 based on orbitals associated with a given electronic configuration.

The main results are collected in Table 3. The calculated Δ_{int} values in Table 3 are consistent with the law embodied in eq 3 showing, in particular, that Δ_{int} just changes sign on passing from $R_{eq} - R_{ax} = 0.15$ Å to $R_{eq} - R_{ax} = -0.15$ Å. A value $\beta = 2.8$ eV/Å for $R_m = 2.05$ Å is derived from the present calculations.

As it is shown in Table 3, the charges transferred to 2pσ orbitals are, as expected, higher than those corresponding to 2s orbitals. However, when the tetragonality increases, the relative variation of $q_{p\sigma}^{eq}(b)$ or $q_{p\sigma}^{eq}(a)$ quantities is much smaller than that of $q_s^{eq}(b)$ or $q_s^{eq}(a)$ associated with 2s(F) orbitals. For instance, on passing from the octahedral situation ($R_{eq} = R_{ax} = 2.05$ Å) to $R_{eq} = 1.95$ Å and $R_{ax} = 2.25$ Å, $q_s^{eq}(b)$ increases by 55% while $q_{p\sigma}^{eq}(b)$ changes only by 2% and thus it remains nearly constant.

The quantities $q_s^{eq}(b)$ and $q_{p\sigma}^{eq}(b)$ are deeply related to the isotropic (A_s) and anisotropic (A_p) superhyperfine constants, respectively, for *elongated* CuF_6^{4-} units formed in Cu^{2+}-doped fluoroperovskites as a result of a static Jahn−Teller effect.[30,32] Low-temperature electron paramagnetic resonance data indicate that whereas for $CsCdF_3$:Cu^{2+} $A_s = 160$ (5) MHz,[32] it clearly increases up to $A_s = 183$ (5) MHz[30] for $KZnF_3$:Cu^{2+}. By contrast, the measured values $A_p = 76$ (5) MHz for $CsCdF_3$:Cu^{2+} and $A_p = 68$ (5) MHz for $KZnF_3$:Cu^{2+} are coincident within experimental uncertainties. This fact is consistent with results for elongated NiF_6^{5-} species in different fluoroperovskites[72,73] involving the $3d^9$ ion Ni^+, where A_s and $q_s^{eq}(b)$ are highly sensitive to the actual value of R_{eq} but not A_p or $q_{p\sigma}^{eq}(b)$. Indeed, whereas A_p changes only by 3% along the series of fluoroperovskites, the variation of A_s is 1 order of magnitude higher (30%).

In the same vein as for octahedral NiF_6^{4-}, MnF_6^{4-}, or FeF_6^{3-} units in cubic fluoroperovskites,[54,74−79] both A_s and q_s quantities, corresponding to the $e_g(\sigma)$ orbital, are strongly dependent upon the metal−ligand distance, while A_p is much less sensitive.

These facts already suggest that, according to eq 15, the gap Δ_{int} is mainly due to the $\Delta_{int}(s)$ contribution reflecting changes in the 3d−2s admixture when the tetragonality increases. This idea is certainly reinforced looking at results of present calculations embodied in Table 3. Indeed, such results prove that the obtained $\Delta_{int}(s)$ contribution essentially accounts for the calculated gap Δ_{int} at different values of R_{eq} and R_{ax} distances. For instance, for $R_{eq} = 1.95$ Å and $R_{ax} = 2.25$ Å, the results of Table 3 give $\Delta_{int}(p\sigma) = -0.10$ eV and $\Delta_{int}(s) = -0.86$ eV. Therefore, comparing these values with the figure $\Delta_{int} = -0.84$ eV derived from DFT calculations, we can conclude that such a gap is greatly the result of variations of the 3d−2s admixture with the tetragonality. Although this conclusion may be surprising, we can note that, from results of Table 3 for $R_{eq} = 1.95$ Å and $R_{ax} = 2.25$ Å, it is verified that

$$q_s^{eq}(b)/q_{p\sigma}^{eq}(b) = 0.225 > (E_d - E_{2p})^2/(E_d - E_{2s})^2$$

$$= 0.066 \tag{17}$$

just implying that

$$\langle d_b|h - E_d|\chi_s^{eq}(b)\rangle^2 \cong 3.4 \langle d_b|h - E_d|\chi_{p\sigma}^{eq}(b)\rangle^2 \tag{18}$$

Thus, the coupling of the 2s-ligand wavefunction, $\chi_s^{eq}(b)$, with $|d_b\rangle = |x^2 - y^2\rangle$ is a little stronger than that for the 2p-wavefunction, $\chi_p^{eq}(b)$. This conclusion is qualitatively consistent with the Wolfsberg−Helmholz guess[80] used before the arrival of ab initio calculations.

Bearing eq 3 in mind, we have also explored the dependence of Δ_{int} and the β quantity upon the average value of the metal−ligand distance, R_m. Varying R_m in the range 1.95−2.05 Å we have found that Δ_{int} and β are sensitive to the value of R_m according to the law

$$\delta\Delta_{int}/\Delta_{int} = \delta\beta/\beta = -4(\delta R_m/R_m) \tag{19}$$

We have verified that the increase of Δ_{int} and β when R_m decreases is also followed by an increase of the $Q_s(a) - Q_s(b)$ quantity while the contribution of $Q_{p\sigma}(a) - Q_{p\sigma}(b)$ is again much less sensitive to the change of R_m. This situation is thus akin to that described in Table 3.

4.2. Variation of 10Dq with the Metal−Ligand Distance for Octahedral Complexes.
Bearing the present results and those previously obtained[67] on O_h complexes in mind, we want now to explain quantitatively the origin of the dependence of 10Dq on the metal−ligand distance, R.

Experimental values for a variety of octahedral complexes[54,61,67,79] lead to an R dependence of the intrinsic contribution to 10Dq, $(10Dq)_{int}$, given by[54]

$$(10Dq)_{int} = KR^{-t} \tag{20}$$

where the exponent t usually lies in the 4−6 range and thus it is close to the value $t = 5$ provided by CF theory.[17]

According to previous results, $(10Dq)_{int}$ can reasonably be approximated by[67]

$$(10Dq)_{int} \cong (10Dq)_{int}(p) + (10Dq)_{int}(s) \tag{21}$$

where the ratio $\alpha = (10Dq)_{int}(s)/(10Dq)_{int}$ has been found to be around 0.65[67] for the series of CrX_6^{3-} units (X = F, Cl, Br,

I). Similarly to results of Section 4.1, the changes of $(10Dq)_{int}$ due to R variations are essentially driven by the $(10Dq)_{int}(s)$ contribution, reflecting the dependence of the q_s charge of 2s, 3s, 4s, or 5s ligand orbitals on the metal−ligand distance.

Thus, writing

$$q_s = CR^{-t_s} \tag{22}$$

and considering small R variations ($\delta R \ll R$), the following quantitative relation among t, t_s, and α comes out

$$t = t_s \alpha \tag{23}$$

Values of the exponent t_s in the 6.5−8.5 range have been derived for doped cubic fluorides[54,67,76,79] and are responsible for the high sensitivity of the isotropic superhyperfine constant, A_s, to R variations well observed experimentally.[54,74−79]

For Mn^{2+}-doped cubic fluoroperovskites, a value $t_s = 8$ has been obtained,[76] while from the parallel study of optical spectra,[81] $t = 4.7$ is found. These values are thus consistent with eq 23 and $\alpha \approx 0.6$.

Despite this fact and the early work by Sugano and Shulman,[16,17] proving that $(10Dq)_{int}$ essentially reflects the different covalent bonding in $e_g(\sigma)$ and $t_{2g}(\pi)$ levels, experimental values of the exponent t close to 5 are still taken as a support to the validity of CF theory.[40]

The sensitivity of 10Dq to R variations has a useful application for changing the shape of the fluorescence band in fluorides doped with Cr^{3+}. Indeed, while the emission spectrum at ambient pressure of both Cr^{3+}-doped $KZnF_3$ and K_2NaGaF_6 lattices is a broad band arising from the $^4T_2$ excited state, a sharp ruby-like spectrum coming from a ^2E first excited state is detected for pressures smaller than 15 GPa.[82,83]

4.3. Key Role of Deep 2s(F) Orbitals in Chemical Bonding and the 2p(F)−2s(F) Gap: Microscopic Origin.
The big separation, $\varepsilon(2p) - \varepsilon(2s) \cong 23$ eV, between 2p and 2s levels of both free fluorine atom and the negative F^- ion,[27−29] cannot be ascribed to a different extent of such orbitals. If we denote by $R_{2p}(r)$ and $R_{2s}(r)$ the radial functions of 2p and 2s orbitals and by $R_{1s}(r)$ that of the inner 1s orbital, in Figure 2
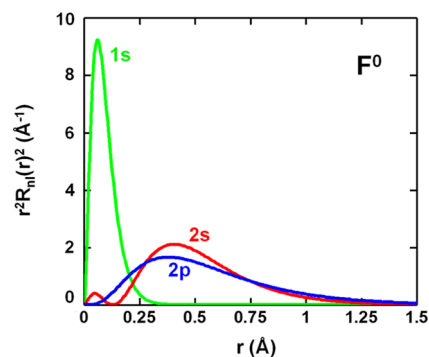

Figure 2. Radial probability densities $P_j(r) = r^2R_j^2(r)$ (j = 1s, 2s, 2p) corresponding to free fluorine atom calculated by means of the atomic wavefunctions of Bunge et al.[29]

are depicted the radial probability densities $P_j(r) = r^2R_j^2(r)$ (j = 1s, 2s, 2p) corresponding to free fluorine atom. While the maximum of $P_{1s}(r)$ is reached for $r_{1s} = 0.06$ Å, those for 2p and 2s orbitals both appear at higher distances but are very close. Indeed, as shown in Figure 2, the maximum of $P_{2p}(r)$ is at $r_{2p} = 0.36$ Å and that of $P_{2s}(r)$ at $r_{2s} = 0.40$ Å. It should be noted however that, when $r > 0.75$ Å, $P_{2p}(r)$ is always a bit higher

than $P_{2s}(r)$. This situation is consistent with the calculated overlap integrals $S_{p\sigma}$ and S_s for a series of octahedral MF_6 complexes[65] (M = Ni^{2+}, Co^{2+}, Mn^{2+}, Fe^{3+}, Cr^{3+}, Mn^{4+}). Indeed, at equilibrium distances, $S_{p\sigma}$ and S_s are both around 0.1 although $S_{p\sigma}$ is a little higher than S_s. Nevertheless, due to the longer tail of the 2p orbital when compared to the 2s wavefunction (Figure 2), the dependence of S_s upon the metal−ligand distance is stronger[73] than that of $S_{p\sigma}$.

The behavior of radial 2p and 2s wavefunctions depicted in Figure 2 is also consistent with the fact that the matrix elements $\langle d_b | h - E_d | \chi_{p\sigma}^{eq} \rangle$ and $\langle d_b | h - E_d | \chi_s^{eq} \rangle$ involved in eq 18 are comparable. Indeed, they just reflect that both functions look rather similar when $r > 0.5$ Å.

Thus, if the extent of 2p and 2s orbitals is comparable, it is now necessary to understand why $\varepsilon(2p) - \varepsilon(2s) \cong 23$ eV for fluorine, while that gap is strictly equal to zero for the hydrogen atom and hydrogenic ions such as He^+ or Li^{2+}.

It should first be stressed that the degeneracy between 2p and 2s orbitals in hydrogen is far from being accidental. In fact, it is the result of an invariant quantity, which appears however only when the potential energy, $U(r)$, seen by the electron is strictly Coulombian[84] and thus has the form

$$U(r) = -Ze^2/r \tag{26}$$

at every distance r from the nucleus.

When this condition is fulfilled, in addition to the angular momentum, $\mathbf{L}$, the so-called Runge−Lenz operator, $\mathbf{A}$, also commutes with the Hamiltonian of the problem.[84] The expression of that operator is given by

$$\mathbf{A} = (1/2\mu)[(\mathbf{p} \wedge \mathbf{L}) - (\mathbf{L} \wedge \mathbf{p})] - Ze^2(\mathbf{r}/r) \tag{27}$$

where μ means the reduced mass of the hydrogen atom. The $\mathbf{A}$ operator connects the radial $R_{2s}(\mathbf{r})$ and $R_{2p}(\mathbf{r})$ wavefunctions and thus implies that the corresponding levels are to be degenerate. This operator was used by Pauli[85] for solving the energy spectrum of the hydrogen atom in the framework of the matrix quantum mechanics by Heisenberg and Born.

The Runge−Lenz vector also plays a relevant role in studying the motion of planets around the sun. Its invariance implies that the position of the perihelion remains constant in time.[86]

In an atom different from H or ions such as He^+ or Li^{2+}, the self-consistent potential felt by a valence electron is not described by eq 26 in the whole range of distances to the nucleus as the net charge, Ze, seen by the electron depends on the r value. Therefore, for the fluorine atom, when $r \ll r_{1s}$, $Z \cong 9$, whereas when $r_{1s} < r < r_{2s}$, Z would be around 7 due to the screening by two inner electrons.

Bearing these facts in mind, the origin of the big separation between 2p and 2s levels in fluorine atom stems from the different behavior of the wavefunctions in the internal $r < 0.1$ Å region. As shown in Figure 2, $P_{2s}(r)$ has a small maximum at r_M = 0.04 Å with $P_{2s}(r_M) = 0.4$ Å^{-1}. By contrast, $P_{2p}(r)$ is essentially zero in the $0 < r < 0.1$ Å region as a result of the $l(l + 1)/r^2$ term in the radial equation making that $R_{2p}(0) = 0$ but $R_{2s}(0) \neq 0$. Thus, the 2s charge $P_{2s}(r_M)\Delta r = 0.02e$ for $\Delta r = 0.05$ Å implies an energy gain for the 2s orbital with respect to the 2p one in that internal region, which can be estimated to be ~ 20 eV using the virial theorem and $Z = 7$. It is worth noting that, if the 2p−2s separation in F mainly arises from the distinct behavior of both wavefunctions in the internal region, it is also consistent with a $\varepsilon(2p) - \varepsilon(2s)$ value for F$^-$ that is

only 5% higher than for the fluorine atom.[27,61] In the same vein, the value of $\varepsilon(np) - \varepsilon(ns)$ for Cl$^-$ (n = 3) and Br$^-$ (n = 4) ions is only 2% higher than that for the corresponding free atom.[27,61]

These considerations thus account for the big $\varepsilon(2p) - \varepsilon(2s)$ value for fluorine and explain the fact that $q_s^{eq}(b) \ll q_{p\sigma}^{eq}(b)$. Moreover, due to the similar extent of the radial 2p and 2s wavefunctions when $r > 0.5$ Å, we can understand that the bonding with deeper 2s(F) orbitals is not negligible.

Nevertheless, it is surprising that the value of the Δ_{int} gap essentially arises from the 3d−2s admixture rather than from the 3d−2p one despite $q_s^{eq}(b) \ll q_{p\sigma}^{eq}(b)$. However, from eq 15 and the results embodied in Table 3, this surprising conclusion is fully consistent with the near independence of $q_{p\sigma}^{eq}(b)$ charges on the $R_{ax} - R_{eq}$ value describing the tetragonal distortion. By contrast, $q_s^{eq}(b)$ increases by 55% on passing from $R_{eq} = R_{ax} = 2.05$ Å to the D_{4h} geometry corresponding to $R_{eq} = 1.95$ Å and $R_{ax} = 2.25$ Å (Table 3).

This situation is thus akin to that encountered for the antibonding e_g orbitals of octahedral complexes.[54,79] Therefore, for the $e_g(x^2 - y^2)$ orbital, $q_{p\sigma}^{eq}$ is again found to be higher than q_s^{eq} but the dependence of q_s^{eq} on the metal ligand distance, R, is much stronger than that of $q_{p\sigma}^{eq}$.

This important result has been explained[54,73,79] considering that $\lambda_{p\sigma}^{eq}(e_g)$ depends on the ratio $\langle d(x^2 - y^2)|h - E_d|\chi_{p\sigma}^{eq}\rangle/(E_d - E_p)$. Accordingly, when R is reduced, the quantity $|\langle d(x^2 - y^2)|h - E_d|\chi_{p\sigma}^{eq}\rangle|$ increases roughly following the corresponding overlap integral $S_{p\sigma}$. However, this increase is compensated by the additional rise of the charge-transfer excitation $E_d - E_p$ due to the lessening of the metal−ligand distance on an isolated 3d complex.[54,73,87] By contrast, in the case of the admixture with the deeper 2s(F) orbital, the variation of q_s^{eq} with the distance essentially reflects that of $[S_s(R)]^2$. Examples of this behavior are shown in refs.[73,76,79]

5. FINAL REMARKS

The present work highlights that the relation between spectroscopic data of TM compounds with the chemical bonding can be very subtle.

When in an isolated CuF_6^{4-} complex, we move from an initial octahedral situation ($\eta = 0$) to a tetragonal one with $\eta \neq 0$ the energy of eigenstates and thus Δ_{int} are modified. There are two sources of that change: (a) the dependence on η of the Hamiltonian and (b) the additional dependence on the distortion of the associated wavefunctions. The present analysis supports that the main contribution to Δ_{int} arises from the variations undergone by $b_{1g}(\sim x^2 - y^2)$ and $a_{1g}(\sim 3z^2 - r^2)$ wavefunctions when η is modified and thus the center of the gravity theorem[88] cannot be applied. Furthermore, Δ_{int} is essentially associated with the variations experienced by the 2s(F) charge with η because the 2pσ(F) charge is nearly independent of the tetragonal distortion.

The present ideas can also be useful for understanding 3d complexes where fluorine is replaced by other halides or oxygen as ligand. Indeed, for these ligands, the $\varepsilon(np) - \varepsilon(ns)$ gap is also significant and lies in the 14−18 eV range.[61] Taking as a guide the case of CdCl$_2$:Cu^{2+}, the tetragonal splitting, Δ_{int}, has been measured[89] to be equal to -0.79 eV as a result of a static Jahn−Teller effect, leading to an elongated octahedral geometry. As there are no available data on the equilibrium geometry of the CuCl$_6^{4-}$ unit in CdCl$_2$, we have derived it through first-principles calculations giving $R_{eq} = 2.33$ Å and $R_{ax} = 2.63$ Å. On this basis, we obtain for CuCl$_6^{4-}$ in CdCl$_2$ a value

β = 2.6 eV/Å that is comparable to that reported in Section 4.1 for the isolated CuF_6^{4-} unit. Furthermore, using these calculated R_{eq} and R_{ax} values in the CF expression for Δ_{int} given in eq 5, we obtain for $CdCl_2$:Cu^{2+} a value Δ_{int}(CF) = −0.12 eV, thus stressing the inadequacy of the CF approach.

From results of Section 4.1 the gap, Δ_{int}, increases significantly upon applied pressures. This fact can be of interest in the realm of superconductor oxocuprates where the transition temperature, T_c, is related[53] to the value of such a gap.

Although the ground state of MnF_6^{4-} and CrF_6^{3-} units in cubic lattices is orbitally singlet, this is no longer true for T_{1g} and T_{2g} excited states[90] where there is a coupling with the Jahn−Teller mode, e_g, well seen through the progressions in luminescence spectra.[91] From calculations carried out on MnF_6^{4-}, Δ_{int} = 0.147 eV for $R_{ax} - R_{eq}$ = −0.06 Å was obtained,[90] thus implying β = 2.46 eV/Å. This figure is thus similar to that derived for the ground state of tetragonal CuF_6^{4-} units that also involves a divalent cation.

Electronic levels lying far from the HOMO play also an important role in the realm of structural instabilities.[92] Therefore, due to the admixture of the ground with excited states via the electron-vibration coupling, the NH_3 molecule is non-planar[93−95] and an orthorhombic distortion appears in A_2CuF_4 (A = K, Na)[4,9,49] and NH_4Cl:$CuCl_4(H_2O)_2^{2-}$[51] but not in NH_4Cl:$CuCl_4(NH_3)_2^{2-}$.[96] In the same vein, isolated Mn^+ ions in KCl:Mn^+[97] or Cu^{2+} in $SrCl_2$:Cu^{2+}[54] move spontaneously from the cubic site to an off-center position, a situation not found in $BaTiO_3$ for an *isolated* Ti^{4+} ion, stressing that ferroelectricity involves a *cooperative* distortion of all Ti^{4+} ions.[97] Interestingly, the value of the excitation involved in the instability of the ammonia molecule goes up to 12 eV[94,95] although it is usually smaller for other systems[51] such as NH_4Cl:$CuCl_4(H_2O)_2^{2-}$.

■ AUTHOR INFORMATION

Corresponding Author

 J. A. Aramburu − *Departamento de Ciencias de la Tierra y Física de la Materia Condensada, Universidad de Cantabria, 39005 Santander, Spain;* ⊙ orcid.org/0000-0002-5030-725X; Email: aramburj@unican.es

Author

 M. Moreno − *Departamento de Ciencias de la Tierra y Física de la Materia Condensada, Universidad de Cantabria, 39005 Santander, Spain*

Complete contact information is available at:
https://pubs.acs.org/10.1021/acs.jpca.0c11609

Notes

The authors declare no competing financial interest.

■ ACKNOWLEDGMENTS

■ REFERENCES

(1) Powell, R. C. *Physics of Solid-State Laser Materials*; Springer-Verlag: New York, 1998.

(2) Bebenin, N. G.; Zainullina, R. I.; Ustinov, V. V. Colossal magnetoresistance manganites. *Phys. Usp.* **2018**, *61*, 719−738.

(3) Hord, R.; Cordier, G.; Hoffmann, K.; Buckow, A.; Pascua, G.; Luetkens, H.; Alff, L.; Albert, B. Enhanced two-dimensional behavior of metastable T′-La₂CuO₄, the parent compound of electron-doped cuprate superconductors. *Phys. Rev. B: Condens. Matter Mater. Phys.* **2010**, *82*, No. 180508(R).

(4) García-Fernández, P.; Moreno, M.; Aramburu, J. A. Electrostatic control of orbital ordering in noncubic crystals. *J. Phys. Chem. C* **2014**, *118*, 7554−7561.

(5) Li, X.; Zhong, X.; Hu, Y.; Li, B.; Sheng, Y.; Zhang, Y.; Weng, C.; Feng, M.; Han, H.; Wang, J. Organic−inorganic copper(II)-based material: A low-toxic, highly stable light absorber for photovoltaic application. *J. Phys. Chem. Lett.* **2017**, *8*, 1804−1809.

(6) Cortecchia, D.; Dewi, H. A.; Yin, J.; Bruno, A.; Chen, S.; Baikie, T.; Boix, P. P.; Grätzel, M.; Mhaisalkar, S.; Soci, C.; Mathews, N. Lead-free MA₂CuClₓBr₄₋ₓ hybrid perovskites. *Inorg. Chem.* **2016**, *55*, 1044−1052.

(7) Jaffe, A.; Karunadasa, H. I. Lithium cycling in a self-assembled copper chloride−polyether hybrid Eeectrode. *Inorg. Chem.* **2014**, *53*, 6494−6496.

(8) Jaffe, A.; Lin, Y.; Mao, W. L.; Karunadasa, H. I. Pressure-induced conductivity and yellow-to-black piezochromism in a layered Cu−Cl hybrid perovskite. *J. Am. Chem. Soc.* **2015**, *137*, 1673−1678.

(9) Aramburu, J. A.; García-Fernández, P.; Mathiesen, N. R.; Garcia-Lastra, J. M.; Moreno, M. Changing the usual interpretation of the structure and ground state of Cu²⁺-layered perovskites. *J. Phys. Chem. C* **2018**, *122*, 5071−5082.

(10) Bosi, F.; Belardi, G.; Ballirano, P. Structural features in Tutton's salts K₂[M²⁺ (H₂O)₆] (SO₄)₂, with M²⁺ = Mg, Fe, Co, Ni, Cu, and Zn. *Am. Mineral* **2009**, *94*, 74−82.

(11) Colaneri, M. J.; Teat, S. J.; Vitali, J. Electron paramagnetic resonance characteristics and crystal structure of a Tutton salt analogue: copper-doped cadmium creatininium sulfate. *J. Phys. Chem. A* **2020**, *124*, 2242−2252.

(12) Aramburu, J. A.; Bhowmik, A.; García-Lastra, J. M.; García-Fernández, P.; Moreno, M. Insight into compounds with Cu-(H₂O)₆²⁺units: new ideas for understanding Cu²⁺ in Tutton salts. *J. Phys. Chem. C* **2019**, *123*, 3088−3101.

(13) Colaneri, M. J.; Vitali, J. Probing axial water bound to copper in Tutton salt using single crystal ¹⁷O-ESEEM spectroscopy. *J. Phys. Chem. A* **2018**, *122*, 6214−6224.

(14) García-Fernández, P.; Moreno, M.; Aramburu, J. A. Origin of the exotic blue color of copper-containing historical pigments. *Inorg.Chem.* **2015**, *54*, 192−199.

(15) Capobianco, N. La couleur de vitraux au XII siècle. Etude chimique et spectroscopique. PhD Thesis, Sorbonne Université, 2019.

(16) Sugano, S.; Shulman, R. G. Covalency effects in KNiF₃. III.Theoretical studies. *Phys. Rev.* **1963**, *130*, 517−530.

(17) Sugano, S.; Tanabe, Y.; Kamimura, H. *Multiplets of Transition-Metal Ions in Crystals*; Academic Press: New York, 1970.

(18) Ballhausen, C. *Molecular Electronic Structures of Transition Metal Complexes*; McGraw-Hill, 1979.

(19) Dyson, F. A meeting with Enrico Fermi. *Nature* **2004**, *427*, 297.

(20) Atanasov, M.; Ganyushin, D.; Sivalingam, K.; Neese, F. A modern first-principles view on ligand field theory through the eyes of correlated multireference wavefunctions. *Struct. Bonding* **2012**, *143*, 149−220.

(21) García-Lastra, J. M.; Barriuso, M. T.; Aramburu, J. A.; Moreno, M. Cr³⁺ in layered perovskites: do the electron paramagnetic resonance parameters only depend on the impurity−ligand distances? *J. Phys.: Condens. Matter* **2010**, *22*, 155502.

(22) Hoggard, P. E. Angular Overlap Model Parameters. *Struct. Bonding* **2004**, *106*, 37−57.

(23) Aramburu, J. A.; Garcia-Fernandez, P.; García-Lastra, J. M.; Barriuso, M. T.; Moreno, M. Internal electric fields and color shift in Cr³⁺-based gemstones. *Phys. Rev. B: Condens. Matter Mater. Phys.* **2012**, *85*, 245118.

(24) Aramburu, J. A.; García-Fernández, P.; García-Lastra, J. M.; Moreno, M. Jahn−Teller and non-Jahn−Teller systems involving

CuF_6^{4-} units: role of the internal electric field in $Ba_2ZnF_6:Cu^{2+}$ and other insulating systems. *J. Phys. Chem. C* **2017**, *121*, 5215−5224.

(25) García-Lastra, J. M.; Aramburu, J. A.; Barriuso, M. T.; Moreno, M. Impurities in non cubic crystals: stabilization mechanisms for Jahn-Teller ions in layered perovskites. *Phys. Rev. Lett.* **2004**, *93*, 226402.

(26) Hunault, M. O. J. Y.; Harada, Y.; Miyawaki, J.; Wang, J.; Meijerink, A.; de Groot, F. M. F.; van Schooneveld, M. M. Direct observation of Cr^{3+} 3d States in ruby: toward experimental mechanistic evidence of metal chemistry. *J. Phys. Chem. A* **2018**, *122*, 4399−4413.

(27) Clementi, E.; Roetti, C. Roothaan-Hartree-Fock atomic wavefunctions. *At. Data Nucl. Data Tables* **1974**, *14*, 177−478.

(28) Moore, C. E. *Atomic Energy Levels*; National Bureau of Standards: Washington D.C. 35, 1971.

(29) Bunge, C. F.; Barrientos, J. A.; Bunge, A. V. Roothaan-Hartree-Fock Ground-State Atomic Wave Functions: Slater-Type Orbital Expansions and Expectation Values for Z = 2-54. *At. Data Nucl. Data Tables* **1993**, *53*, 113−162.

(30) Minner, E. M. C. Etude spectroscopique des ions Jahn-Teller cuivre et argent bivalents dans des monocristaux de fluoroperovskites de composition chimique AMF3. Ph.D. Thesis, University of Geneva, Switzerland, 1993.

(31) Dubicki, L.; Riley, M. J.; Krausz, E. R. Electronic-structure of the copper(ii) ion doped in cubic $KZnF_3$. *J. Chem. Phys.* **1994**, *101*, 1930−1938.

(32) Minner, E.; Lovy, D.; Bill, H. Electron-paramagnetic-resonance and relaxation study of copper(ii) and silver(ii) in $CsCdF_3$ single-crystals. *J. Chem. Phys.* **1993**, *99*, 6378−6383.

(33) Borcherts, R. H.; Kanzaki, H.; Abe, H. EPR spectrum of a Jahn-Teller system, $NaCl-Cu^{2+}$. *Phys. Rev. B: Solid State* **1970**, *2*, 23−27.

(34) Ham, F. S. Jahn−Teller Effects in EPR Spectra. In *Electron Paramagnetic Resonance*; Geschwind, S., Ed.; Plenum: New York, 1972.

(35) Garcia-Fernandez, P.; Trueba, A.; Barriuso, M. T.; Aramburu, J. A.; Moreno, M. Dynamic and static Jahn-Teller effect in impurities: determination of the tunneling splitting. *Prog. Theor. Chem. Phys.* **2011**, *23*, 105−142.

(36) García-Fernández, P.; Trueba, A.; Barriuso, M. T.; Aramburu, J. A.; Moreno, M. Tunneling splitting of Jahn-Teller ions in oxides. *Phys.Rev. Lett.* **2010**, *104*, 035901.

(37) McLain, S. E.; Dolgos, M. R.; Tennant, D. A.; Turner, J. F. C.; Barnes, T.; Proffen, T.; Sales, B. C.; Bewley, R. I. Magnetic behaviour of layered Ag(II) fluorides. *Nat. Mater* **2006**, *5*, 561−565.

(38) Kurzydłowski, D.; Jaroń, T.; Ozarowski, A.; Hill, S.; Jagličić, Z.; Filinchuk, Y.; Mazej, Z.; Grochala, W. Local and cooperative Jahn−Teller Effect and resultant magnetic properties of M_2AgF_4 (M = Na−Cs). *Inorg. Chem.* **2016**, *55*, 11479−11489.

(39) Reinen, D. The modulation of Jahn-Teller coupling by elastic and binding strain perturbations-a novel view on an old phenomenon and examples from solid-state chemistry. *Inorg.Chem.* **2012**, *51*, 4458−4472.

(40) Candela, M. T.; Jara, E.; Aguado, F.; Valiente, R.; Rodríguez, F. Structural correlations in Jahn-Teller systems of Mn^{3+} and Cu^{2+}: unraveling local structures through spectroscopic techniques. *J. Phys. Chem. C* **2020**, *124*, 22692−22703.

(41) Li, W. M.; et al. Superconductivity in a unique type of copper oxide. *Proc. Natl. Acad. Sci. USA* **2019**, *116*, 12156−12160.

(42) Wingefeld, G.; Hoppe, R. Über $KCuAlF6$. *Z. Anorg. Allg. Chem.* **1984**, *516*, 223.

(43) Finnie, K.; Dubicki, L.; Krausz, E. R.; Riley, M. J. Spectroscopic verification of a tetragonal compression in an octahedral copper(II) compound. *Inorg. Chem.* **1990**, *29*, 3908−3910.

(44) Mazej, Z.; Arčon, I.; Benkič, P.; Kodre, A.; Tressaud, A. Compressed octahedral coordination in chain compounds containing divalent copper: structure and magnetic properties of $CuFAsF_6$ and $CsCuAlF_6$. *Chem.—Eur. J.* **2004**, *10*, 5052−5058.

(45) Aramburu, J. A.; Moreno, M. Ground State and Optical Excitations in Compounds with tetragonal CuF_6^{4-} units: insight into $KAlCuF_6$ and $CuFAsF_6$. *Inorg. Chem.* **2020**, *59*, 539−547.

(46) Riley, M. J.; Dubicki, L.; Moran, G.; Krausz, E. R.; Yamada, I. Absorption and magnetic circular-dichroism spectra of the compressed copper(II) ion in K_2ZnF_4. *Chem. Phys.* **1990**, *145*, 363−373.

(47) Reinen, D.; Steffen, G.; Hitchman, M. A.; Stratemeier, H.; Dubicki, L.; Krausz, E. R.; Riley, M. J.; Mathies, H. E.; Recker, K.; Wallrafen, F. The optical-spectrum of Ba_2ZnCuF_6. *Chem. Phys.* **1991**, *155*, 117−125.

(48) Aramburu, J. A.; Moreno, M. Understanding the structure and ground state of the prototype CuF_2 compound not due to the Jahn−Teller effect. *Inorg. Chem.* **2019**, *58*, 4609−4618.

(49) Sanchez-Movellan, I.; Aramburu, J. A.; Moreno, M. Local structure and excitations in systems with CuF_6^{4-} units: lack of Jahn−Teller effect in the low symmetry compound Na_2CuF_4. *Phys. Chem. Chem. Phys.* **2020**, *22*, 7875−7887.

(50) Boettcher, F.; Spaeth, J. M. ENDOR Investigation of Cu^{2+} Centres in NH_4Cl. *Phys. Status Solidi B* **1974**, *61*, 465−473.

(51) Garcia-Fernandez, P.; Garcia-Lastra, J. M.; Trueba, A.; Barriuso, M. T.; Aramburu, J. A.; Moreno, M. Insulators containing $CuCl_4X_2^{2-}(X = H_2O, NH_3)$ units: origin of the orthorhombic distortion observed only for $CuCl_4(H_2O)_2^{2-}$. *Phys. Rev. B: Condens. Matter Mater. Phys.* **2012**, *85*, 094110.

(52) García-Fernández, P.; Barriuso, M. T.; García-Lastra, J. M.; Moreno, M.; Aramburu, J. A. Compounds containing tetragonal Cu^{2+} complexes: is the d_{x2-y2}- d_{3z2-r2} gap a direct reflection of the distortion? *J. Phys. Chem. Lett.* **2013**, *4*, 2385−2390.

(53) Sakakibara, H.; Usui, H.; Kuroki, K.; Arita, R.; Aoki, H. Origin of the material dependence of Tc in the single-layered cuprates. *Phys. Rev. B: Condens. Matter Mater. Phys.* **2012**, *85*, 064501.

(54) Moreno, M.; Barriuso, M. T.; Aramburu, J. A.; García-Fernández, P.; García-Lastra, J. M. Microscopic insight into properties and electronic instabilities of impurities in cubic and lower symmetry insulators: Influence of pressure. *J. Phys.: Condens. Matter* **2006**, *18*, R315−R360.

(55) Brik, M. G. 3d ions in solids and microscopic crystal field effects: theoretical analysis and relations with experimental spectroscopic data. *IOP Conf. Ser.: Mater. Sci. Eng.* **2020**, *835*, 012032.

(56) García-Lastra, J. M.; Barriuso, M. T.; Aramburu, J. A.; Moreno, M. Origin of the different color of ruby and emerald. *Phys. Rev. B: Condens. Matter Mater. Phys.* **2005**, *72*, 113104.

(57) Gaudry, E.; Kiratisin, A.; Sainctavit, P.; Brouder, C.; Mauri, F.; Ramos, A.; Rogalev, A.; Goulon, J. Structural and electronic relaxations around substitutional Cr^{3+} and Fe^{3+} ions in corundum. *Phys. Rev. B: Condens. Matter Mater. Phys.* **2003**, *67*, 094108.

(58) Gaudry, E.; Cabaret, D.; Brouder, C.; Letard, I.; Rogalev, A.; Wilhlem, F.; Jaouen, N.; Sainctavit, P. Relaxations around the substitutional chromium site in emerald: x-ray absorption experiments and density functional calculations. *Phys. Rev. B: Condens. Matter Mater. Phys.* **2007**, *76*, 094110.

(59) Low, W.; Suss, J. T. Jahn-Teller Effect of Ni^+ and Cu^{2+} in single crystals of calcium oxide. *Phys. Lett.* **1963**, *7*, 310−312.

(60) Aramburu, J. A.; García-Fernández, P.; García-Lastra, J. M.; Moreno, M. A genuine Jahn-Teller system with compressed geometry and quantum effects originating from zero-point motion. *ChemPhysChem* **2016**, *17*, 2146−2156.

(61) Moreno, M.; Aramburu, J. A.; Barriuso, M. T. Electronic properties and bonding in transition metal complexes: influence of pressure. *Struct. Bonding* **2004**, *106*, 127−152.

(62) Fraga, S.; Karwowski, J.; Saxena, K. M. S. *Handbook of Atomic Data*; Elsevier: Amsterdam, 1976.

(63) Löwdin, P. O. A Note on the quantum−mechanical perturbation theory. *J. Chem. Phys* **1951**, *19*, 1396−1401.

(64) McWeeny, R.; Sutcliffe, B. T. *Methods of Molecular Quantum Mechanics*; Academic Press: New York, 1969; p 36.

(65) Davies, J. J.; Smith, S. R. P.; Owen, J.; Hann, B. F. ENDOR measurements of spin transfer in $(VF_6)^{4-}$. *J. Phys. C: Solid State Phys.* **1972**, *5*, 245−256.

(66) Parr, R. G.; Yang, W. *Density-Functional Theory of Atoms and Molecules*; Oxford University Press: New York, 1989.

(67) Trueba, A.; Garcia-Fernandez, P.; García-Lastra, J. M.; Aramburu, J. A.; Barriuso, M. T.; Moreno, M. Spectrochemical series and the dependence of Racah and 10Dq parameters on the metal-ligand distance: microscopic origin. *J. Phys. Chem. A* 2011, 115, 1423−1432.

(68) Barriuso, M. T.; Aramburu, J. A.; Moreno, M. Puzzling absence of hyperfine interaction in the D_{4h} $RhCl_6^{4+}$ centre: role of the 4d−5s hybridization in Rh^{2+} centres. *J. Phys.: Condens. Matter* 2002, 14, 6521−6530.

(69) te Velde, G.; Bickelhaupt, F. M.; Baerends, E. J.; Fonseca Guerra, C.; van Gisbergen, S. J. A.; Snijders, J. G.; Ziegler, T. Chemistry with ADF. *J. Comput. Chem.* 2001, 22, 931−967.

(70) Becke, A. D. Density-functional thermochemistry. III. The role of exact exchange. *J. Chem. Phys.* 1993, 98, 5648−5652.

(71) Vetere, V.; Adamo, C.; Maldivi, P. Performance of the 'parameter free' PBE0 functional for the modeling of molecular properties of heavy metals. *Chem. Phys. Lett.* 2000, 325, 99−105.

(72) Zorita, E.; Alonso, P. J.; Alcalá, R. Tetragonal Ni ions in x-ray-irradiated $KMgF_3$:Ni. *Phys. Rev. B: Condens. Matter Mater. Phys.* 1987, 35, 3116−3121.

(73) Aramburu, J. A.; Moreno, M.; Barriuso, M. T. How do the electronic properties of d^9 impurities depend on metal-ligand distances? Application to Ni^+, Cu^{2+} and Ag^{2+} Systems. *J. Phys.: Condens.Matter* 1992, 4, 9089−9112.

(74) Villacampa, B.; Cases, R.; Orera, V. M.; Alcalá, R. EPR and Optical Study of Ni^{2+} Ions in $CsCaF_3$ and $CsCdF_3$. *J. Phys. Chem. Solids* 1994, 55, 263−272.

(75) Rousseau, J. J.; Leblé, A.; Fayet, J. C. Examen des paramètres de l'Hamiltonien de spin de Mn^{2+} substitue a M, dans les fluoperovskites AMF_3, dans la phase tetragonale de $RbCaF_3$ et dans les composés A_2MF_4. *J. Phys.* 1978, 39, 1215−1223.

(76) Barriuso, M. T.; Moreno, M. Determination of the Mn^{2+}-F^- distance from the isotropic superhyperfine constant for $[MnF_6]^{4+}$ in ionic lattices. *Phys. Rev. B: Condens. Matter Mater. Phys.* 1984, 29, 3623−3631.

(77) DuVarney, R. C.; Niklas, J. R.; Spaeth, J. M. ENDOR study of Fe^{3+} centres in $KMgF_3$. *Phys. Status Solidi B* 1981, 103, 329−336.

(78) Dance, J. M.; Grannec, J.; Tressaud, A.; Moreno, M. ESR Investigation of phase transitions in some elpasolite-type fluorides. *Phys. Status Solidi B* 1992, 173, 579−586.

(79) Aramburu, J. A.; Paredes, J. I.; Barriuso, M. T.; Moreno, M. Local relaxation around Fe^{3+} in fluorides: influence on electronic properties. *Phys. Rev. B: Condens. Matter Mater. Phys.* 2000, 61, 6525−6534.

(80) Ballhausen, C. J.; Gray, H. B. *Molecular Orbital Theory*; Benjamin: New York, 1965.

(81) Rodriguez, F.; Moreno, M.; Tressaud, A.; Chaminade, J. P. Mn^{2+} in cubic perovskites: determination of the Mn^{2+} −F^- distance from the optical-spectrum. *Cryst. Lattice Defects Amorphous Mater.* 1987, 16, 221−225.

(82) Freire, P. T. C.; Pilla, O.; Lemos, V. Pressure-induced level crossing in $KZnF_3$:Cr^{3+}. *Phys. Rev. B: Condens. Matter Mater. Phys.* 1994, 49, 9232−9235.

(83) Dolan, J. F.; Rinzler, A. G.; Kappers, L. A.; Bartram, R. H. Pressure and temperature dependence of chromium photoluminescence spectra in fluoride elpasolites. *J. Phys. Chem. Solids* 1992, 53, 905−912.

(84) Galindo, A.; Pascual, P. *Quantum Mechanics I*; Springer-Verlag: Berlin, 1990.

(85) Pauli, W. Über das Wasserstoffspektrum vom Standpunkt der neuen Quantenmechanik. *Zeit. Physik.* 1926, 36, 336−363.

(86) Rañada, A. *Dinámica Clásica*; Alianza Editorial: Madrid, 1990; p 302.

(87) Aramburu, J. A.; Moreno, M.; Bencini, A. Charge-transfer transitions in $CuCl_4^{2-}$ and $CuBr_4^{2-}$ complexes: dependence on the metal-ligand distance. *Chem. Phys. Lett.* 1987, 140, 462−467.

(88) Ballhausen, C. J. *Introduction to Ligand Field Theory*; McGraw-Hill: New York, 1962.

(89) Kan'no, K.; Mukai, S.; Nakai, Y. Vibronically allowed d-d transitions of Cu^{2+} centers in $CdCl_2$ and $CdBr_2$. *J. Phys. Soc. Japan* 1974, 36, 1492.

(90) Barriuso, M. T.; Aramburu, J. A.; Moreno, M. Coupling with the Jahn-Teller mode for triplet states of MF_6 (M = Mn^{2+}, Cr^{3+}) complexes: dependence on the M-F distance and influence on the Stokes shift. *Phys. Status Solidi B* 1996, 196, 193−208.

(91) Wenger, O. S.; Güdel, H. U. Optical spectroscopy of $CrCl_6^{3-}$ doped $Cs_2NaScCl_6$: Broadband near-infrared luminescence and Jahn-Teller effect. *J. Chem. Phys* 2001, 114, 5832−5841.

(92) Bersuker, I. B. Pseudo-Jahn−Teller effect. a two-state paradigm in formation, deformation, and transformation of molecular systems and solids. *Chem. Rev.* 2013, 113, 1351−1390.

(93) García-Fernández, P.; Aramburu, J. A.; Moreno, M.; Zlatar, M.; Gruden-Pavlović, M. A practical computational approach to study molecular instability using the pseudo Jahn−Teller effect. *J. Chem. Theory Comput.* 2014, 10, 1824−1833.

(94) Wedler, H. B.; Wendelboe, P.; Tantillo, D. J.; Power, P. P. Second order Jahn−Teller interactions at unusually high molecular orbital energy separations. *Dalton Trans.* 2020, 49, 5175−5182.

(95) Bersuker, I. B.; Gorinchoi, N. N.; Polinger, V. Z. On the origin of dynamic instability of molecular systems. *Theor. Chim. Acta* 1984, 66, 161−172.

(96) Breñosa, A. G.; Moreno, M.; Rodriguez, F.; Couzi, M. Evidence for anomalous relaxation of the $CuCl_4(NH_3)_2^{2-}$ center in NH_4Cl below T_c. *Phys. Rev. B: Condens. Matter Mater. Phys.* 1991, 44, 9859−9863.

(97) García-Lastra, J. M.; García-Fernández, P.; Calle-Vallejo, F.; Trueba, A.; Aramburu, J. A.; Moreno, M. Quantifying local and cooperative components in the ferroelectric distortion of $BaTiO_3$: Learning from the off-center motion in the $MnCl_6^{5-}$ complex formed in KCl:Mn^+. *Inorg. Chem.* 2014, 53, 6534−6543.